Surgical and Radiologic Anatomy (2019) 41:1045–1051
https://doi.org/10.1007/s00276-019-02290-z

ORIGINAL ARTICLE

# Possible cerebrospinal fluid pathways in the middle fossa floor and pterional diploe: a magnetic resonance imaging study

**Satoshi Tsutsumi[1] · Hideo Ono[2] · Yukimasa Yasumoto[1] · Hisato Ishii[1]**

Received: 19 May 2019 / Accepted: 11 July 2019 / Published online: 16 July 2019


## Abstract

**Purpose** There has not been a study documenting the distribution of cerebrospinal fluid (CSF) pathways in the anterolateral base of the middle fossa (ALB) and diploe of the pterional region (Pt). The present study aimed to delineate these pathways using magnetic resonance imaging.

**Methods** Thin-sliced, axial, and coronal T2-weighted sequences were performed for a total of 358 outpatients, including 20 pediatric patients.

**Results** *Adult population*: CSF-filled channels were identified on axial images in the ALB in 57% and in the diploe of the Pt in 65% of 338 patients. These pathways showed variable morphology and number bilaterally. CSF-filled channels were identified on coronal images in the ALB in 14% and in the diploe of the Pt in 100% of 59 patients. These were delineated as linear structures of variable number and thickness. Eleven percent of the pathways identified in the ALB was connected with extracranial channels. *Pediatric population*: CSF-filled channels were identified on axial images in the ALB in 75% and in the diploe of the Pt in 80% of 20 patients.

**Conclusions** The ALB and diploe of the Pt may function as CSF pathways in children and adults. The pathways in the ALB can be a CSF-drainage route connecting to the extracranial sites.

**Keywords** Cerebrospinal fluid · Middle fossa · Diploe · Glymphatic

## Introduction

The greater sphenoid wing is a part of the sphenoid bone that forms the anterolateral base of the middle cranial fossa. It is pierced by several foramina that allow the passage of venous channels connecting the interior of the cranium and the extracranial veins [22, 23]. The greater wing can be affected by diverse pathologies, such as primary and metastatic tumors [2, 9, 10, 12, 16, 19, 24], cysts [17, 21, 25], dural arteriovenous fistula [8], and agenesis [20]. The pterion is an important cranial landmark located where the frontal, greater wing of the sphenoid, parietal, and squamous part of the temporal bone meet. The localization and shape of the pterion have been extensively investigated because it is a useful anatomical landmark for various surgical approaches and interventions [1, 4, 15, 18].

Cerebrospinal fluid (CSF) dynamics are still not completely understood. Studies have suggested that intracranial CSF may flow into the deep cervical lymph nodes via the dural lymphatic network or glymphatic system [3, 6, 7, 11, 13]. However, morphology of these pathways connecting the intra- and extracranial sites has not been demonstrated using neuroimaging. Our preliminary examination using magnetic resonance imaging (MRI) indicated that these CSF pathways might be distributed in the anterolateral base of the middle fossa (ALB) and pterional region (Pt). These regions, which are situated relatively close to each other on the inner surface of the cranium, have not been studied in association with CSF pathways (Fig. 1).

The aim of the present study was to explore the distribution of these pathways in the ALB and Pt using thin-sliced, T2-weighted MRI.

✉ Satoshi Tsutsumi
shotaro@juntendo-urayasu.jp

[1] Department of Neurological Surgery, Juntendo University Urayasu Hospital, 2-1-1 Tomioka, Urayasu, Chiba 279-0021, Japan

[2] Division of Radiological Technology, Medical Satellite Yaesu Clinic, Tokyo, Japan

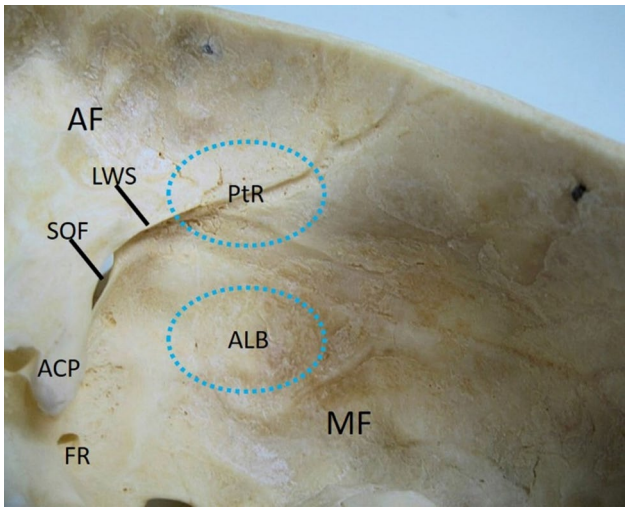


**Fig. 1** The right half of a dry human skull, viewed from the posterosuperior aspect, showing the inner surface of the anterolateral base of the middle fossa (ALB) and pterional region (Pt) located relatively close to each other, in the cranium (areas within dotted circles) *ACP* anterior clinoid process, *AF* anterior fossa, *ALB* anterolateral base of the middle fossa, *FR* foramen rotundum, *LWS* lesser wing of the sphenoid, *MF* middle fossa, *PtR* inner surface of the pterional region, *SOF* superior orbital fissure

## Materials and methods

The present study included a total of 358 outpatients who visited our hospital between November 2009 and June 2015. These patients had headaches, dizziness, vertigo, tinnitus, hearing disturbances, hemisensory disturbances, and seizures. The sample consisted of 173 men and 185 women, with a mean age of 50 years (range 8–81 years). Among them, 20 were pediatric patients under the age of 18 years, including 13 boys and 7 girls. Initial examinations with axial T1- and T2-weighted images, T2-gradient echo, fluid-attenuated inversion recovery, and diffusion-weighted sequences confirmed that none of the patients had previous intracranial hemorrhage, brain tumors, traumatic brain injury accompanying skull fractures, hydrocephalus, or cysts. Then, these patients underwent examination with thin-sliced, axial T2-weighted sequences involving the whole cranial base and calvarial vault. Fifty-nine of the 338 adult patients underwent additional coronal T2-weighted imaging. For each T2 sequence, the following parameters were used: repetition time, 3500.0 ms; echo time, 90.0 ms; slice thickness, 2.0 mm; interslice gap, 0 mm; matrix, 300 × 189; field-of-view, 200 mm × 200 mm; flip angle, 90°; and scan duration, 2 min 40 s. All sequences were obtained using a 3.0-T MR scanner (Achieva R2.6, Philips Medical Systems; Best, The Netherlands). Imaging data were transferred to a workstation (Virtual Place Lexus 64, 64 edition; AZE; Tokyo, Japan) and analyzed independently by two authors (S.T. and H.I.). When a high-intensity structure identified in the ALB and Pt was clearly continuous with the intracranial subarachnoid spaces at its medial-most part, the structure was judged to be a CSF-filled channel and was recorded for analysis. High-signal morphologies confusing with the linings of air sinuses and fat tissue in the diploe were excluded.

The study was performed in accordance with our institution's guidelines for human research. Written informed consent was obtained from all patients prior to their participation.

## Results

Three hundred and fifty-eight patients were divided into adult and pediatric populations. The former included 338 patients and the latter 20 patients. Outcomes were analyzed separately for each population.

### Adult population

CSF-filled channels were identified on axial images in the ALB in 194 of 338 patients (57%), on the right side in 144 patients (43%), and on the left side in 157 (46%) patients. These channels were delineated as fine and multiple canals varying in morphology and number, bilaterally (Fig. 2). Moreover, CSF-filled channels were identified in the diploe of the Pt in 219 patients (65%), on the right side in 190 patients (56%), and on the left side in 201 (59%) patients. A majority of the channels had linear structures of variable thickness, with a consistent posterior course (Fig. 3). On coronal imaging, CSF pathways were identified in the ALB in 8 of 59 patients (14%), on the right side in 4 patients (7%), and on the left side in 6 (10%) patients. These pathways commonly showed vesicular dilations just below the middle fossa floor (Fig. 4). The pathways were also identified in the diploe of the Pt in 59 (100%) patients, on the right side in 44 patients (75%), and on the left side in 54 (92%) patients. These pathways had linear structures of variable number and thickness, coursing upward along the pterional diploe (Fig. 5). In 37 patients (11%), the CSF pathways in the ALB were found to connect to the extracranial pathways, branching in the medial, lower, and upper directions, as observed on serial axial and coronal images (Fig. 6). The identification ratios of CSF pathways in the ALB and diploe of the Pt are summarized in Table 1.

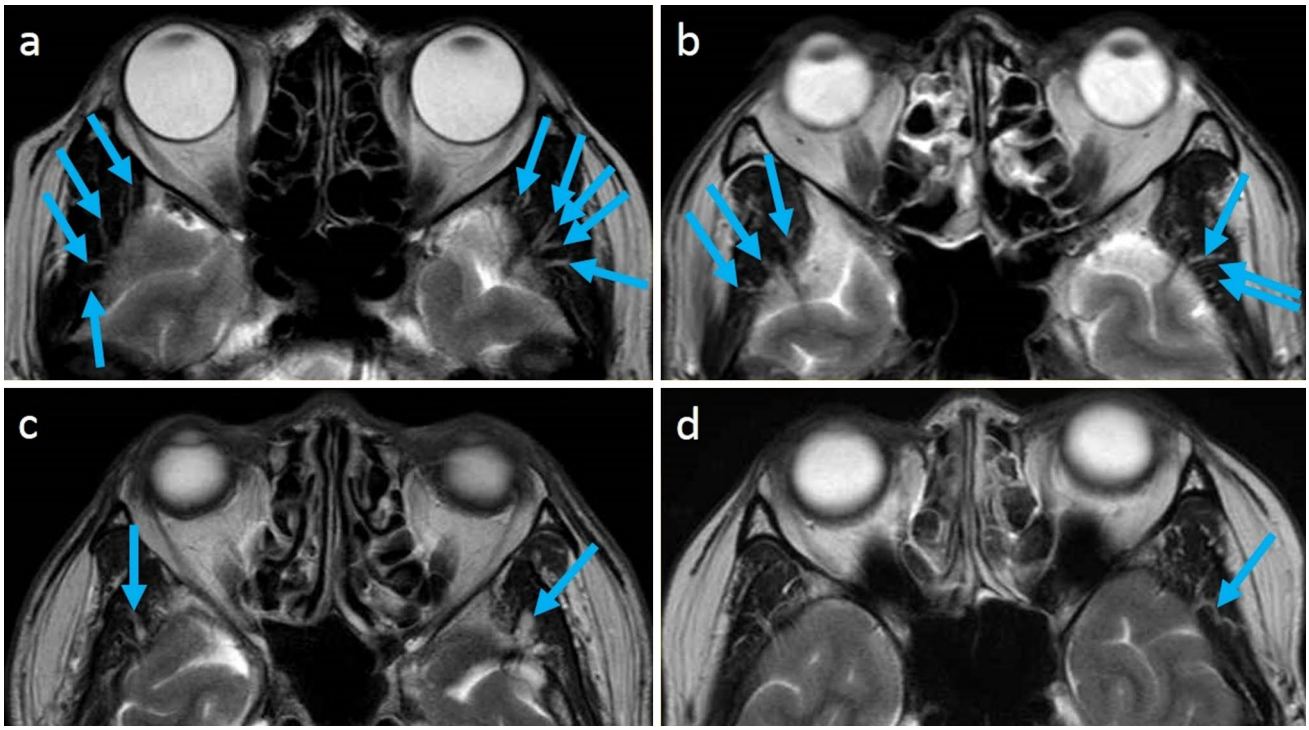


**Fig. 2** **a–d** Axial T2-weighted magnetic resonance images of different adult patients showing cerebrospinal fluid-filled channels in the anterolateral base of the middle fossa, identified as fine and multiple canals with variable morphology and number, bilaterally (arrows)

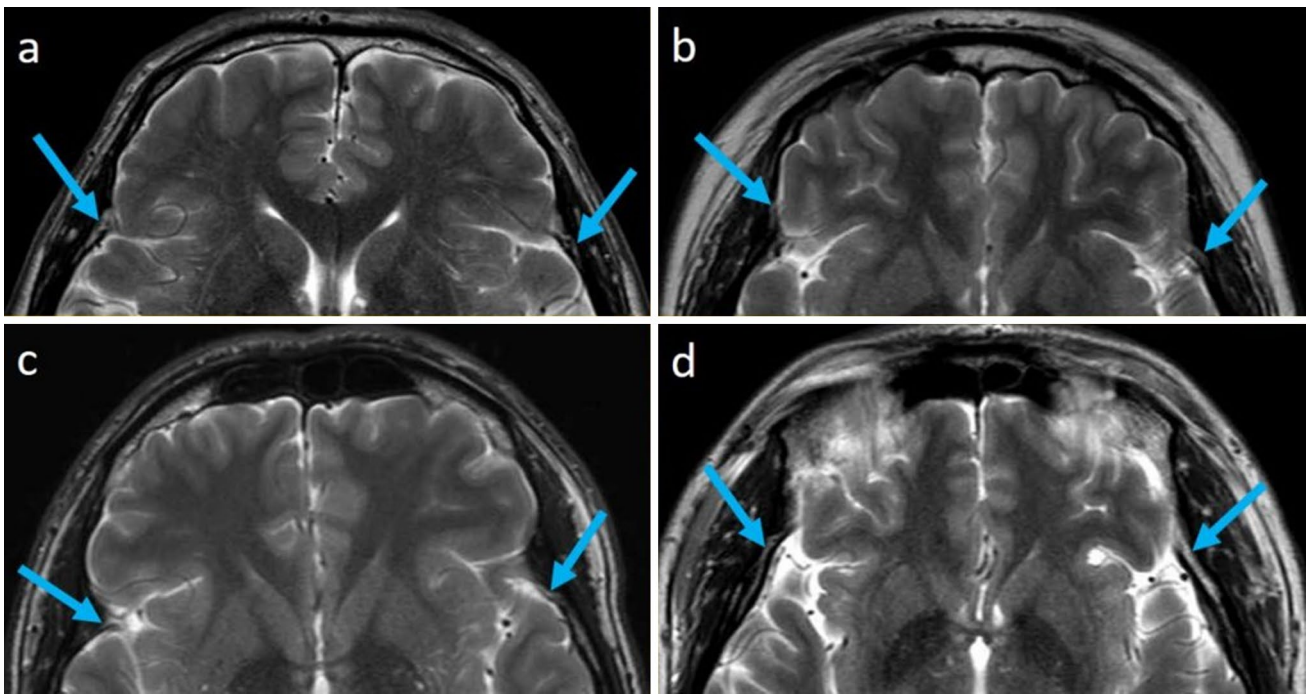


**Fig. 3** **a–d** Axial T2-weighted magnetic resonance images of different adult patients showing linear morphology of the cerebrospinal fluid-filled channels in the diploe of the pterional region with variable thickness, with a consistent posterior course (arrows)

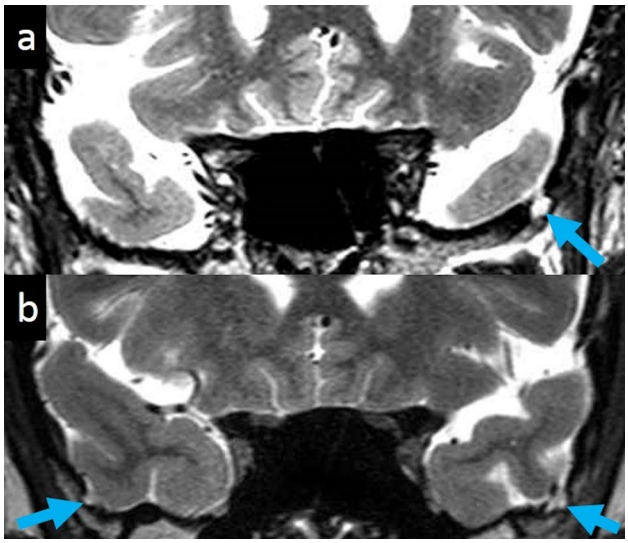


**Fig. 4** **a**, **b** Coronal T2-weighted magnetic resonance images of different adult patients showing cerebrospinal fluid-filled channels in the anterolateral base of the middle fossa, showing vesicular dilations just below the floor (arrows)

### Pediatric population

All the pediatric patients were examined using thin-sliced, axial T2-weighted sequence. The CSF pathways were identified in the ALB in 15 of 20 patients (75%), on the right side in 12 patients (60%) and on the left side in 11 (55%) patients. These CSF pathways showed variable morphology and number on both sides. They were also identified in the diploe of the Pt in 16 (80%), on the right side in 14 patients (70%) and on the left side in 14 (70%) patients (Table 1). A majority of these pathways were linear, with varying locations and thicknesses in the Pt, with a consistent posterior course (Fig. 7). A summary of the CSF pathways recorded in pediatric patients is listed in Table 2.

## Discussion

In the present study, CSF-filled channels were identified on axial images in the ALB in 57% and in the diploe of the Pt in 65% of the adult population. They were identified in the ALB in 14% and in the diploe of the Pt in 100% of the adult population on coronal images. These discrepancies in the identification ratios between the two sequences seemed to arise mainly due to the fineness and peculiarity of the shapes of the CSF pathways, distributed in the ALB and Pt. At the ALB, these pathways commonly coursed almost horizontally, while they coursed in an upward direction in the pterional diploe. Furthermore, in 11% of adult patients, the pathways identified in the ALB were connected with extracranial channels. These extracranial channels may function as a part of the glymphatic system, which needs further investigation in a quantitative manner.

Notably, CSF pathways were identified in 75% in the ALB and in 80% in the diploe of the Pt in the pediatric population of the present study, where they were more frequently identified than the adult population. This may indicate that these two regions are important locations in the human cranium that help in the drainage of intracranial CSF into extracranial sites, probably functioning throughout life. The reason for the abundant presence of the CSF pathways in the ALB and

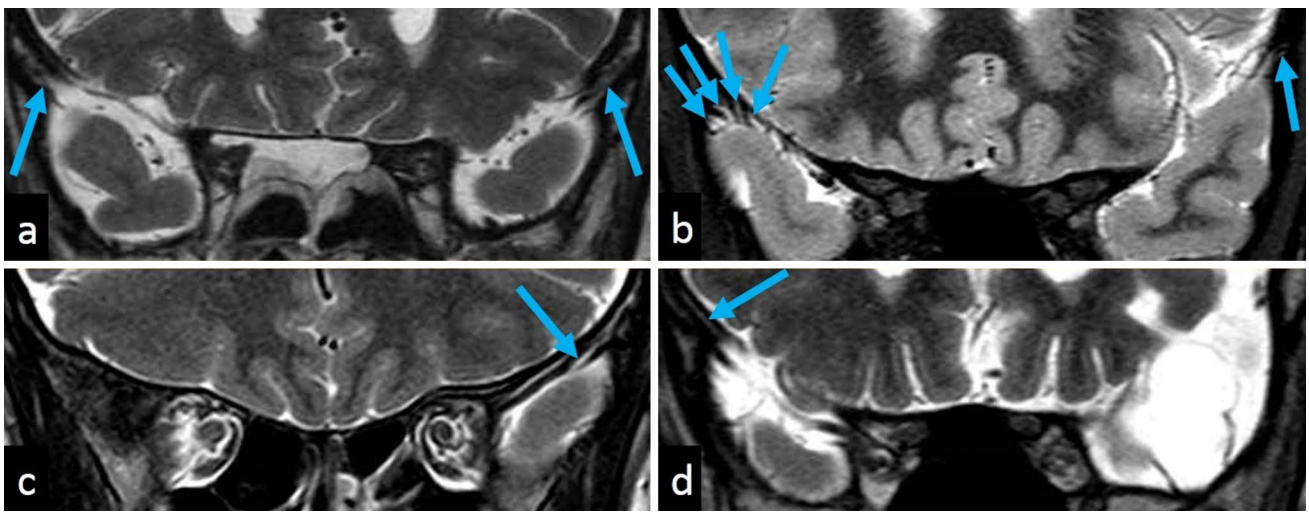


**Fig. 5** **a–d** Coronal T2-weighted magnetic resonance images of different adult patients showing cerebrospinal fluid-filled channels in the diploe of the pterional region presenting variable number and thickness, bilaterally, and coursing upward (arrows). Morphological changes in the left temporal lobe identified in (**d**) is an old cerebral infarct

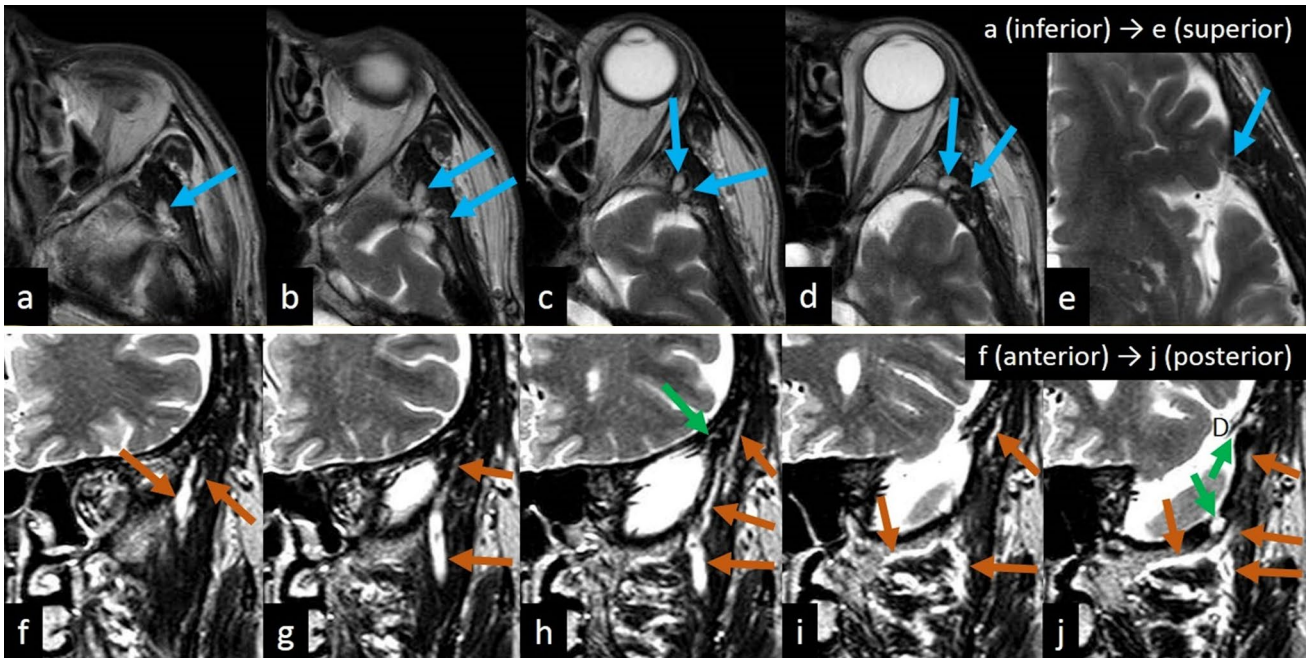


**Fig. 6** Serial axial (**a–d**), coronal (**f–j**), and axial (**e**) T2-weighted magnetic resonance images of an adult patient showing cerebrospinal fluid-filled channels in the left anterolateral base of the middle fossa (**a–d** blue arrows; **j** lower green arrow) and diploe of the pterional region (**e** blue arrow; **j** upper green arrow). Extracranial cerebrospinal fluid-filled channels, with inhomogeneous diameters and irregular branching patters, are delineated on coronal images, communicating with the subarachnoid space of the anterolateral base of the middle fossa floor (**j** lower green arrow), and branching in the medial, lower, and upper directions (**f–j** brown arrows). *D:* dura mater (color figure online)

**Table 1** Summary of the identification ratios in adult and pediatric populations

| | Axial | Images | Coronal | Images |
|---|---|---|---|---|
| | Adult | Pediatric | Adult | Pediatric |
| ALB | 194/338 (57%)<br>(R: 144 (43%); L: 157 (46%)) | 15/20 (75%)<br>(R: 12 (60%); L: 11 (55%)) | 8/59 (14%)<br>(R: 4 (7%); L: 6 (10%)) | 0 |
| DipPt | 219/338 (65%)<br>(R: 190 (56%); L: 201 (59%)) | 16/20 (80%)<br>(R: 14 (70%); L: 14 (70%)) | 59/59 (100%)<br>(R: 44 (75%); L: 54 (92%)) | 0 |

*ALB* anterolateral base of the middle fossa, *DipPt* diploe of the pterional region, *L* left side, *R* right side

Pt needs further investigation to study their embryological, anatomical, and functional implications.

In the present investigation, the T2-weighted sequence was adopted because it well delineated the CSF-filled spaces continuous with the intracranial subarachnoid spaces. However, the sequence did not discriminate the spaces and lining arachnoids. Therefore, these identified structures can be arachnoid granulations, brain herniations into the granulations, or intradiploic encephaloceles, rather than CSF pathways [5, 14]. Despite these possibilities, based on careful observations, we considered that these structures can represent CSF pathways. Studies using the constructive interference in steady-state sequence and fast imaging employing steady-state acquisition, well discriminating the CSF and adjacent neurovascular structures, may verify the validity of the present investigation.

This study has limitations. Our investigation used a retrospective analysis for two different populations. Participants were not randomly assigned to the sample population. The distribution of the subjects in the population, based on age and sex, varied greatly. Furthermore, the pediatric population was much smaller than the adult population. Moreover, the CSF pathways were delineated only on the axial and coronal planes, and their three-dimensional architectures were not assessed. However, we consider these findings helpful for improving our understanding of the CSF pathways connecting the ALB and diploe of the Pt with extracranial pathways in the ALB.

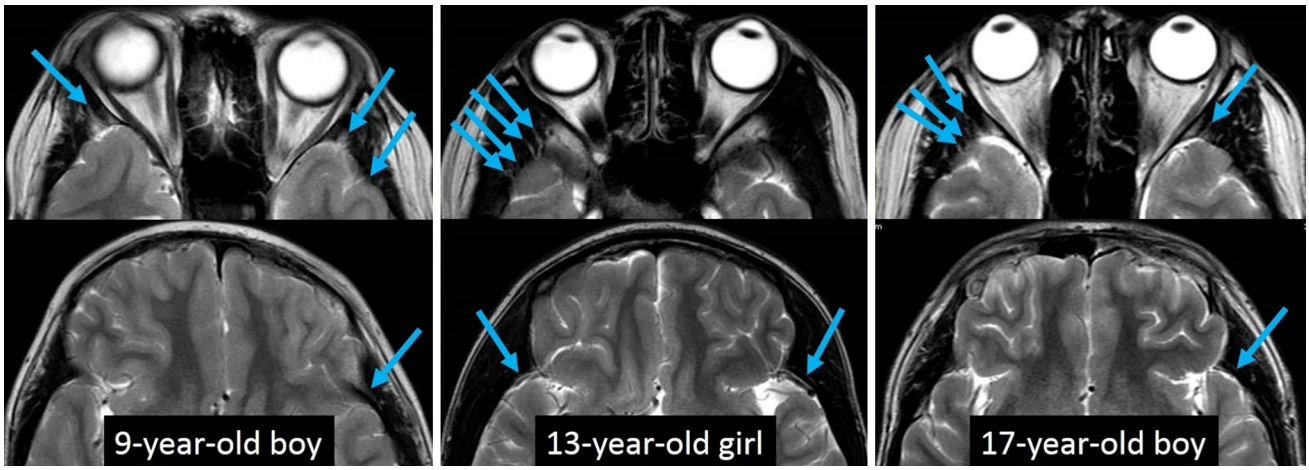


**Fig. 7** Axial T2-weighted magnetic resonance images of three different pediatric patients showing cerebrospinal fluid-filled channels in the anterolateral base of the middle fossa (upper row) and diploe of the pterional region (lower row) with variable morphology and number, bilaterally (arrows)

**Table 2** Summary of CSF pathways in pediatric patients

| Patient no. | Age (years) | Gender | ALB | DipPt |
|---|---|---|---|---|
| 1 | 8 | Boy | L | L |
| 2 | 9 | Boy | R, L | R, L |
| 3 | 9 | Boy | R, L | R, L |
| 4 | 9 | Boy | R | UI |
| 5 | 12 | Boy | L | R, L |
| 6 | 13 | Boy | R, L | R, L |
| 7 | 14 | Boy | UI | UI |
| 8 | 16 | Boy | L | R, L |
| 9 | 16 | Boy | R, L | R, L |
| 10 | 16 | Boy | UI | UI |
| 11 | 17 | Boy | R, L | R, L |
| 12 | 17 | Boy | UI | R, L |
| 13 | 18 | Boy | UI | UI |
| 14 | 10 | Girl | UI | R, L |
| 15 | 13 | Girl | R | R, L |
| 16 | 13 | Girl | R, L | R |
| 17 | 14 | Girl | R | L |
| 18 | 18 | Girl | R | R, L |
| 19 | 18 | Girl | R, L | R, L |
| 20 | 18 | Girl | R, L | R |

*ALB* anterolateral base of the middle fossa, *DipPt* diploe of the pterional region, *L* left side, *R* right side, *UI* unidentified

## Conclusions

The ALB and diploe of the Pt may function as CSF pathways in both, pediatric and adult populations. The pathways in the ALB can be a CSF-drainage route connecting to the extracranial sites.

**Acknowledgements** This work was not supported by grant funding.

**Author contributions** All the authors contributed equally to the study. ST conceived the study design. HI and YY collected the imaging data. HO and HI analyzed the imaging data. ST wrote the manuscript.

## Compliance with ethical standards

**Conflict of interest** The authors have no conflicts of interest concerning the materials or methods used in this study, or the findings presented in this paper.

## References

1. Aksu F, Akyer SP, Kale A, Geylan S, Gayretli O (2014) The localization and morphology of pterion in adult West Anatolian skulls. J Craniofac Surg 25:1488–1491
2. Apostolopoulos K, Ferekidis E (2003) Extensive primary Ewings' sarcoma in the greater wing of the sphenoid bone. ORL J Otorhinolaryngol Relat Spec 65:235–237
3. Aspelund A, Antila S, Proulx ST, Karlsen TV, Karaman S, Detmar M, Wiig H, Alitalo K (2015) A dural lymphatic vascular system that drains brain interstitial fluid and macromolecules. J Exp Med 212:991–999
4. Aydin ME, Kopuz C, Demir MT, Corumlu U, Kaya AH (2010) Localization of pterion in neonatal cadavers: a morphometric study. Surg Radiol Anat 32:545–550
5. Battal B, Hamcan S, Akgun V, Sari S, Oz O, Tasar M, Castillo M (2016) Brain herniations into the dural venous sinus or calvarium: MRI findings, possible causes and clinical significance. Eur Radiol 26:1723–1731
6. Boulton M, Flessner M, Armstrong D, Hay J, Johnston M (1998) Determination of volumetric cerebrospinal fluid absorption into extracranial lymphatics in sheep. Am J Physiol 274:R88–R96
7. Boulton M, Armstrong D, Flessner M, Hay J, Szalai JP, Johnston M (1998) Raised intracranial pressure increases CSF drainage through arachnoid villi and extracranial lymphatics. Am J Physiol 275:R889–R896

8. Cohen JE, Gomori JM, Grigoriadis S, Spektor S, Rajz G (2008) Dural arteriovenous fistula of the greater sphenoid wing region in neurofibromatosis type 1. Pediatr Neurosurg 44:172–175
9. Crisi G, Calo M, Mauri C (1986) Case report 358: desmoid tumor of the greater wing of the right sphenoid bone. Skeletal Radiol 15:247–250
10. De Foer B, Hermans R, Morlion J, Baert AL (1993) Solitary plasmacytoma of the greater wing with secondary submandibular soft tissue metastasis. J Belge Radiol 76:169–170
11. Eide PK, Vatnehol SAS, Emblem KE, Ringstad G (2018) Magnetic resonance imaging provides evidence of glymphatic drainage from human brain to cervical lymph nodes. Sci Rep 8:7194
12. Gupta PK, Mital M, Dwivedi A, Gupta K (2011) Metastasis of greater wing of sphenoid bone in bronchogenic carcinoma: a unusual case report. J Cancer Res Ther 7:195–197
13. Johnston M (2003) The importance of lymphatics in cerebrospinal fluid transport. Lymphat Res Biol 1:41–44
14. Kandemirli SG, Candan S, Bilgin C (2019) Post-traumatic occipital intradiploic encephalocele. World Neurosurg. https://doi.org/10.1016/j.wneu.2019.05.174
15. Ma S, Baillie LJ, Stringer MD (2012) Reappraising the surface anatomy of the pterion and its relationship to the middle meningeal artery. Clin Anat 25:330–339
16. Meel R, Thulkar S, Sharma MC, Jagadesan P, Mohanti BK, Sharma SC, Bakhshi S (2012) Childhood osteosarcoma of greater wing of sphenoid: case report and review of literature. J Pediatr Hematol Oncol 34:e59–e62
17. Nevrekar D, Abdu E, Selden NR (2009) Craniectomy for a bilobed dermoid cyst in the temporal fossa and greater wing of the sphenoid bone. Pediatr Neurosurg 45:46–48
18. Oguz O, Sanli SG, Bozkir MG, Soames RW (2004) The pterion in Turkish male skulls. Surg Radiol Anat 26:220–224
19. Pelaz AC, Llorente Pendás JL, Rodrigo Tapia JP, Suárez Nieto C (2008) Giant cell tumor of the greater wing of the sphenoid: an unusual presentation. J Craniofac Surg 19:822–826
20. Pinna A, Demontis S, Maltese G, Dore S, Carta F (2005) Absence of the greater sphenoid wing in neurofibromatosis 1. Arch Ophthalmol 123:1454
21. Pun A, King JA, Phal PM, Iseli TA (2018) Giant pseudomeningocele of the greater wing of sphenoid. ANZ J Surg 88:E89–E90
22. Reymond J, Charuta A, Wysocki J (2005) The morphology and morphometry of the foramina of the greater wing of the human sphenoid bone. Folia Morphol (Warsz) 64:188–193
23. Rhoton AL Jr (2002) The anterior and middle cranial base. Neurosurgery 51:S273–S302
24. Sharma RR, Netalkar A, Lad SD (2000) Primary Ewing's sarcoma of the greater wing of the sphenoid bone. Br J Neurosurg 14:53–56
25. Urbach H, Jamneala G, Mader I, Egger K, Yang S, Altenmüller D (2018) Temporal lobe epilepsy due to meningoencephaloceles into the greater sphenoid wing: a consequence of idiopathic intracranial hypertension? Neuroradiology 60:51–60